Applied Mathematics E-Notes, 25(2025), 275-285 © ISSN 1607-2510
Available free at mirror sites of http://www.math.nthu.edu.tw/∼amen/

Fractional Advection-Diffusion Equation With Variable Diffusivity: Pollutant Effects Using Adomian Decomposition Method[*]

Shankar Pariyar[‡], Jeevan Kafle[§]

Received 25 June 2024

Abstract

This work applies Adomian's decomposition method (ADM) to solve a one-dimensional fractional advection-dispersion equation with variable diffusivity. The temporal derivative is substituted with a Caputo fractional derivative of order α (where $0 < \alpha \leq 1$), and spatial derivatives with orders β (where $0 < \beta \leq 1$) and γ (where $1 < \gamma \leq 2$) are used. The concentration effects of three pollutants with different diffusivities are examined under constant wind velocity, and it also analyzes how varying fractional derivatives affect the interaction between advection and diffusion. The accuracy of the solutions improves as the fractional order increases, demonstrating the method's effectiveness in modeling complex pollutant dispersion in systems with heterogeneous diffusion and providing insights into systems with memory effects or long-range interactions.

1 Introduction

The advection-diffusion equation (ADE) is a parabolic partial differential equation widely used in environmental science to model the movement and dispersion of pollutants [12, 21]. Advection describes the transport of substances by a moving fluid, while diffusion refers to the movement of molecules from high to low concentration due to a concentration gradient [13, 23]. Fick's law and the principle of mass conservation, ADE also incorporates methods such as fractional Langevin processes, continuous-time random walks, and fractional Brownian motion. These approaches often model more complex pollutant dispersion patterns in aquatic systems and the atmosphere, and the use of fractional calculus improves predictions of pollutant spread [1, 21, 25].

Fractional calculus (FC), which extends classical calculus by incorporating fractional derivatives and integrals, is a valuable tool in many fields of science and engineering. It is particularly useful for understanding diffusion processes in systems with memory effects, fractal media, and heterogeneous environments. Due to its broad range of applications, FC has attracted significant attention across multiple scientific disciplines [2, 11, 19]. The development of fractional diffusion equations, especially in the context of anomalous diffusion, explores non-integer derivative orders in both space and time, revealing how these affect diffusion patterns [5]. The fractional advection-diffusion equation (FADE) has proven especially effective in modeling fluid transport through porous media [23]. This is achieved by replacing the first-order time derivative in the standard diffusion equation with a Liouville-Caputo derivative and substituting the second-order spatial derivative with a Riesz-Feller derivative [25, 26].

El-Sayed et al. [15] developed a model using fractional derivatives (FD) and applied the Adomian Decomposition Method (ADM) to derive an analytical solution. George Adomian (1923–1996) established the ADM, an effective mathematical technique for solving various differential equations (Adomian, 1994). The ADEs traditionally model particle transport but often fail to depict real-world scenarios accurately due to constant diffusivity assumptions. Mainardi [16]; Liu et al. [14] have recently emerged FADEs incorporating (FD) for better representation in heterogeneous and complex media. Bear [4] introduced variable diffusivity,

---

[*] Mathematics Subject Classifications: 65M70, 35R11, 76M25.

[†] Department of Mathematics, Tri-Chandra Multiple Campus, Tribhuvan University, Kathmandu, Nepal

[‡] Central Department of Mathematics, Tribhuvan University, Kirtipur, Kathmandu, Nepal

[§] Corresponding author, Central Department of Mathematics, Tribhuvan University, Kirtipur, Kathmandu, Nepal which has significantly enhanced ADE models, especially for diffusion in heterogeneous materials. Kumar et al. [12] introduced the space-fractional diffusion equation, describing diffusion in non-homogeneous media and fractal geometries, considering sub- or super-diffusion phenomena [17, 22].

2 Preliminaries

Recall that the Riemann Liouville (*R-L*) fractional integral is defined by

$$
{}_a\mathbf{I}_y^\alpha(f(y)) = \frac{1}{\Gamma(\alpha)} \int_a^y (y-t)^{\alpha-1} f(t)dt,
$$

where Γ is the gamma function and a is an arbitrary but fixed base point. The integral is well defined provided f is locally integrable on suitable intervals, and α is a complex number in the half-plane $\mathrm{Re}(\alpha) > 0$.

Property 1 ([19]) ${}_aI_y^\alpha(\lambda(K(y))) = \lambda\,{}_aI_y^\alpha(K(y))$, ${}_aI_y^\alpha(M(y) \pm N(y)) = {}_aI_y^\alpha M(y) \pm {}_aI_y^\alpha N(y))$ *and* ${}_aI_y^\alpha(N(y) \pm M(y))) = {}_aI_y^\alpha(N(y) \pm {}_aI_y^\alpha M(y))$.

Definition 1 ([16]) *The Riemann-Liouville fractional derivative of order $\alpha > 0$ is defined by*

$$
{}_b\mathbf{D}_x^\alpha(v(x)) = \begin{cases} \frac{1}{\Gamma(m-\gamma)} \frac{d^m}{dx^m} \int_b^x (x-t)^{m-\alpha-1} v(t)dt & (m-1) < \alpha < m, \\ \frac{d^m}{dx^m} v(x) & \alpha = m \end{cases}
$$

where $m = \lceil \alpha \rceil$, the ceiling function of α.

Definition 2 ([1]) *The Caputo fractional derivative (FD) is a kind of fractional derivative*

$$
{}_a\mathbf{D}_z^\alpha(f(z)) = \begin{cases} \frac{1}{\Gamma(p-\alpha)} \int_a^z (z-t)^{p-\alpha-1} \frac{d^p}{dz^p} f(t)dt & (p-1) < \alpha < p,\ \alpha \in \mathbb{R}^+,\ p \in \mathbb{N}, \\ \frac{d^p}{dz^p} f(z) & \alpha = p. \end{cases}
$$

Definition 3 ([20]) *The single-parameter Mittag-Leffler function $E_\alpha(x)$ is defined as,*

$$
E_\alpha(x) = \sum_{k=0}^{\infty} \frac{x^k}{\Gamma(\alpha k + 1)}
$$

where α is a complex parameter, and $\Gamma(.)$ is the gamma function.

It is well known that [3] the *R-L* fractional integral exists if the function $f(x)$ belongs to the space $L^1([a,b])$, which implies that $\int_a^b |f(x)|\,dx < \infty$. Additionally, the Liouville-Caputo fractional derivative exists if the function $f(x)$ is absolutely continuous and satisfies the condition

$$
\int_a^x \frac{|f'(t)|}{(x-t)^{1-\alpha}} dt < \infty.
$$

Principal Components of ADM: In the differential equation $Lu + Ru + N(u) = f(x)$, where $L = D^n$ and $D = \frac{d}{dx}$, $N(u)$ is a nonlinear operator, L and R are linear operators. *ADM* expresses $u(x,t)$ as an infinite series:

$$
u(x,t) = \sum_{k=0}^{\infty} u_k(x,t),
$$

and the nonlinear operator $N(u)$ is expanded as A_n are Adomian polynomials depending on $u_0, u_1, u_2, \cdots$,

$$
A_n = \left[\frac{1}{n!} \frac{d^n}{d\lambda^n} N\left(\sum_{i=0}^{n} \lambda^i u_i \right) \right]_{\lambda=0}, \tag{1}
$$

where $N(u)$ represents the nonlinear term such that

$$\begin{aligned}&\textstyle\sum_{k=0}^{\infty} u_k(x,t) = f(x) - L_t^{-1} L_x \left(\sum_{k=0}^{\infty} u_k\right) - L_t^{-1}\left(\sum_{n=0}^{\infty} A_n\right),\\ &\textstyle\sum_{n+1=0}^{\infty} u_{n+1}(x,t) = f(x) - L_t^{-1} L_x \left(\sum_{n=0}^{\infty} u_n\right) - L_t^{-1}\left(\sum_{n=0}^{\infty} A_n\right),\end{aligned} \tag{2}$$

$$\begin{cases} u_0(x,t) = f(x), \\ u_{n+1}(x,t) = L_t^{-1} L_x u_n - L_t^{-1} A_n \qquad \text{for } k = 0,1,2,3,\ldots. \end{cases} \tag{3}$$

We use the recurrence relation to find the first few components, u_0, u_1, u_2, u_3. These are sufficient to form the series for $u(x,t) \approx \sum_{k=0}^{N} u_k(x,t)$. With N being finite, calculating more terms manually is difficult, so we use computer software; however, the series converges quickly, so only a few terms are needed for an approximate solution. For the exact solution, we use $u(x,t) = \lim_{N\to\infty} \sum_{k=0}^{N} u_k(x,t)$. In both cases, the series converges [10] fast. Equations (1) and (3) are used to solve the nonlinear differential equation $u(x,t) = \sum_{k=0}^{N} u_k(x,t)$. The ADM requires $u(x,t)$ to have a continuous derivative, $N(u)$ to be twice continuously differentiable, and all functions to be smooth so that the inverse operators L_t^{-1} and L_x^{-1} are well-defined. L_t and L_x are linear, while $N(u)$ is nonlinear. These conditions guarantee the convergence and accuracy of the ADM [9].

Example 1 *Consider the nonlinear second order homogeneous partial differential equation,*

$$u_t - u_{xx} + u^2 - u = 0 \tag{4}$$

with the initial condition:

$$u(x,0) = \alpha.$$

Using ADM, the differential operators are decomposed, $L_t = \frac{\partial}{\partial t}$, $L_x = \frac{\partial^2}{\partial x^2}$ *and* $N(u) = (u^2 - u)$. *From* (4): $u(x,t) = L_t^{-1}[L_x(u)] - L_t^{-1}[N(u)] + \alpha$. *Let*

$$u = \sum_{k=0}^{\infty} u_k(x,t), \quad N(u) = u^2 - u \quad \text{and} \quad N(u) = \sum_{n=0}^{\infty} A_n.$$

Then

$$\sum_{k=0}^{\infty} u_k(x,t) = L_t^{-1} L_x \sum_{k=0}^{\infty} u_k(x,t) - L_t^{-1} \sum_{n=0}^{\infty} A_n,$$

$$\begin{cases} u_0(x,t) = \alpha, \\ u_{n+1}(x,t) = L_t^{-1} L_x u_n - L_t^{-1} A_n \qquad \text{for } n = 0,1,2,3,\ldots. \end{cases}$$

So we have that

$$u_1 = L_t^{-1} L_x(u_0) - L_t^{-1}(A_0) = (\alpha - \alpha^2).t, \quad u_2 = L_t^{-1} L_x(u_1) - L_t^{-1}(A_1) = \alpha(\alpha-1)(2\alpha-1)\frac{t^2}{2},$$

$$u_3 = \alpha(\alpha-1)(2\alpha-1)(3\alpha-1)\frac{t^3}{3}\cdots.$$

Then

$$u(x,t) \approx \sum_{k=0}^{\infty} u_k = \alpha + \alpha(\alpha-1)t + \alpha(\alpha-1)(1-2\alpha)\frac{t^2}{2} + \cdots.$$

Convergence of Adomian Series for $\alpha = 1$*:*

1. *For* $N = 0$*:*

$$S_0(x,t) = \alpha = 1 \quad \text{and} \quad S_1(x,t) = \alpha + \frac{\alpha(\alpha-1)}{t} = 1.$$

2. *For* $N = 2$*:*

$$S_2(x,t) = \alpha + \alpha(\alpha-1)t + \frac{\alpha(\alpha-1)(1-2\alpha)}{2}t^2 = 1.$$

Summary of Partial Sums for $\alpha = 1$; $N = 0$: $S_0(x,t) = 1$, *for* $N = 1$: $S_1(x,t) = 1$, *for* $N = 2$, $S_2(x,t) = 1$.

Convergence Behavior

For $\alpha = 1$, the series solution $u(x,t)$ converges rapidly since all terms involving t vanish ($\alpha(\alpha-1) = 0$). The partial sums stabilize at $u(x,t) = 1$, indicating effective convergence of the Adomian series to a constant solution for this case. Although the exact solution is unavailable, the Adomian series provides an infinite representation of the solution. Analyzing the partial sums demonstrates that the ADM solution becomes more accurate as additional terms are included, making ADM a reliable approximation method for solving nonlinear PDEs.

3 Fractional Advection Dispersion Equation in Space -Time

The (FADE) for the concentration field $C(\kappa,\zeta)$, with a single spatial variable κ and time ζ,

$$\frac{\partial^\alpha C(\kappa,\zeta)}{\partial \zeta^\alpha} = \mathbb{G}.\frac{\partial^\gamma C(\kappa,\zeta)}{\partial \kappa^\gamma} - \lambda \frac{\partial^\beta C(\kappa,\zeta)}{\partial \kappa^\beta}, \quad 0 \le \kappa \le L, \tag{5}$$

with $0 < \alpha \le 1$, $\beta > 0$, and $\gamma > 0$, such that the pollutant concentration function $C(\kappa,\zeta)$ has its domain defined over the spatial interval $0 \le \kappa \le L$ and for all times $t \ge 0$. The concentration function $C(\kappa,\zeta)$ and its fractional derivatives will fall within the codomain $\mathbb{R}$, given that $C(\kappa,\zeta)$ is a real-valued function. $C(\kappa,\zeta)$ represents the dissolved concentration, $\mathbb{G}$ denotes the dispersion coefficient, and λ signifies the Darcy velocity, where the diffusion and drift velocity are represented, respectively, by the positive constants $\mathbb{G}$ and λ. When the space variable κ and the time variable ζ take modeled by the Fokker-Planck equation, the diffusion and drift velocity adjust accordingly. Now, let's introduce non-dimensional variables and constants by substituting, $x = \frac{\kappa}{L}$ and $t = \frac{\zeta.\lambda}{L}$, $\frac{\partial}{\partial x} = \frac{\partial}{\partial \kappa}.\frac{\partial \kappa}{\partial x} = L\frac{\partial}{\partial \kappa}$ and $\frac{\partial}{\partial t} = \frac{\partial}{\partial \zeta}.\frac{\partial \zeta}{\partial t} = \frac{L}{\lambda}\frac{\partial}{\partial \zeta}$. Substituting $C(\kappa,\zeta)$ with $u(x,t)$ results in the desired form and (5) reduces to

$$\frac{\partial^\alpha u(x,t)}{\partial t^\alpha} = \frac{\mathbb{G}}{\lambda}.\frac{\partial^\gamma u(x,t)}{\partial x^\gamma} - \frac{\partial^\beta u(x,t)}{\partial x^\beta},$$

$$\mathbb{D}_t^\alpha u = \mu \mathbb{D}_x^\gamma u - \mathbb{D}_x^\beta u, \tag{6}$$

for $x, t > 0$ where $\mu = \frac{\mathbb{G}}{\lambda}$, $\mathbb{D}_t = \frac{\partial}{\partial t}$, and $\mathbb{D}_x = \frac{\partial}{\partial x}$, under initial condition $u(x,0) = e^{-x}$. For a diffusion Peclet number $Pe = \frac{1}{\mu}$, a large Peclet number ($Pe > 100$) indicates that the advection term is the dominant transport mechanism. For $Pe \to 0$, diffusion is the dominant mode of mass transport, and advection is minimal. For $Pe = 1$, both advection and diffusion have the same impact on mass transfer and occur at identical periods. For $Pe \to \infty$, mass transfer is dominated by advection and diffusion is minimal. Using condition $u(x,0) = e^{-x}$, we want to solve FADE model (6) in three different scenarios.

3.1 Time Fractional Advection Diffusion Equation

The FADE in time with $\gamma = 2$ and $\beta = 1$

$$\mathbb{D}_t^\alpha u = \mu \mathbb{D}_x^2 u - \mathbb{D}_x u, \qquad x, t > 0. \tag{7}$$

Applying the initial condition $u(x,0) = e^{-x}$, then equation (7) becomes

$$u(x,t) = u(x,0) + \mu D_t^{-\alpha}(D_x^2 u) - D_t^{-\alpha}(D_x u).$$

The solution to $u(x,t)$ may be determined using infinite series and ADM, $u(x,t) = \sum_{m=0}^{\infty} u_m$ recursive relation, $u_0 = u(x,0) = e^{-x}$ and $u_{n+1} = \mu I^\alpha(D_x^2 u_n) + I^\alpha(D_x u_n)$.

$$u_1 = \mu I^\alpha(\mathbb{D}_x^2(u_0)) - I^\alpha(\mathbb{D}_x(u_0)) = \mu I^\alpha(\mathbb{D}_x^2(e^{-x})) - I^\alpha(\mathbb{D}_x(e^{-x})) = \frac{t^\alpha}{\Gamma(\alpha+1)}(\mu+1)e^{-x},$$

$$u_2 = \frac{t^{2\alpha}}{\Gamma(2\alpha+1)}(\mu+1)^2 e^{-x}, \cdots u_m = \frac{t^{m\alpha}}{\Gamma(m\alpha+1)}(\mu+1)^m e^{-x},$$

$$u(x,t) = e^{-x}\sum_{m=0}^{\infty}\frac{t^{m\alpha}}{\Gamma(m\alpha+1)}(1+\mu)^m = e^{-x}E_\alpha((1+\mu)t^\alpha). \tag{8}$$

The single parameter MLF is represented by E_α. The x-axis shows how pollutant concentration varies across different locations in the atmosphere.

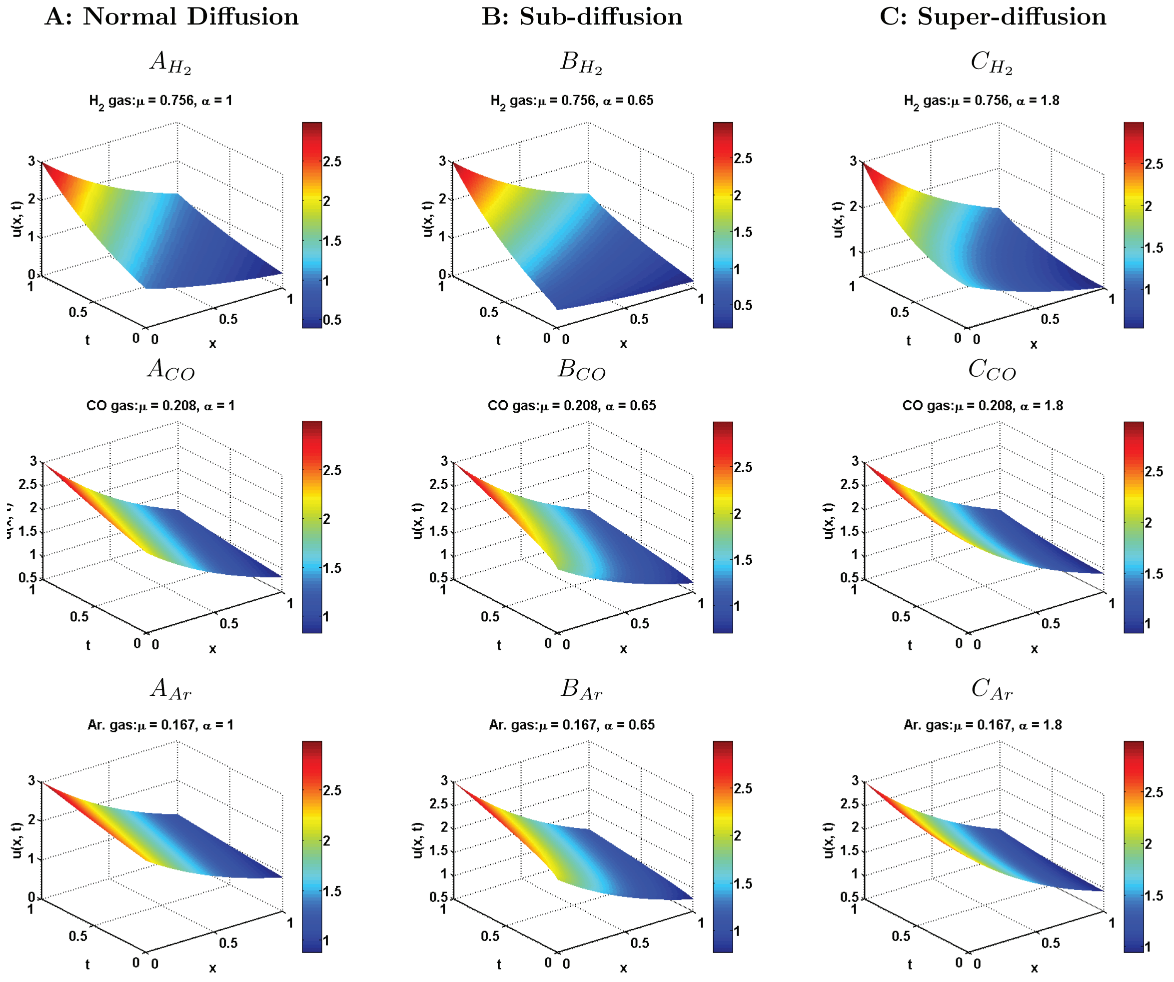

A: Normal Diffusion **B: Sub-diffusion** **C: Super-diffusion**

A_{H_2} B_{H_2} C_{H_2}

A_{CO} B_{CO} C_{CO}

A_{Ar} B_{Ar} C_{Ar}

Figure 1: Comparison of Diffusion Types, A: Normal Diffusion with $\alpha = 1$ for $A_{H_2} : \mu = 0.756$, $A_{CO} : \mu = 0.208$, and $A_{Ar} : \mu = 0.167$; B: Sub-Diffusion with $\alpha = 0.65$ for $B_{H_2} : \mu = 0.756$, $B_{CO} : \mu = 0.208$, and $B_{Ar} : \mu = 0.167$; C: Super-Diffusion with $\alpha = 1.8$ for $C_{H_2} : \mu = 0.756$, $C_{CO} : \mu = 0.208$, and $C_{Ar} : \mu = 0.167$.

Temporal evolution, represented by the y-axis, indicates changes in atmospheric processes and dispersion over time. The concentration of pollutants is depicted on the z-axis. Initially, when pollutants are emitted into the atmosphere, their concentration is higher near the source. As time progresses, these pollutants disperse and spread out, leading to a decrease in concentration near the source and an increase at farther distances. This often results in a peak concentration occurring shortly after the emission. We considered three pollutants: hydrogen gas, carbon monoxide, and argon, with varying diffusivities categorized as high, moderate, and low. These diffusivities are measured at real values of $\mu = 0.756 cm^2/s$, $\mu = 0.208 cm^2/s$, and

$\mu = 0.167 cm^2/s$, respectively in (8), under constant wind velocity conditions at a temperature of 20°C across various orders of fractional derivatives: $\alpha = 1$, 0.65, and 1.8 cf. [18]. In the context of the classical advection-diffusion equation at $\alpha = 1$, pollutants spread consistently according to Fick's laws. Diffusion occurs at a standard rate determined by the concentration gradient and diffusivity coefficient. When $\alpha = 0.65$, pollutants spread more slowly than in normal diffusion, exhibiting sub-diffusion characteristics. This slow diffusion occurs due to impeded movement, leading to long-term memory effects and non-Gaussian behavior, which depart from traditional Fickian diffusion patterns. Superdiffusion occurs when the fractional order of the advection-diffusion equation is $\alpha = 1.8$. This phenomenon indicates a quicker spreading rate compared to classical diffusion. Superdiffusion is observed in systems such as turbulent fluxes and anomalous transport in porous media, where elements cause enhanced mixing, long-range interactions, or active motion. Figures (A_{H_2}, B_{H_2}, C_{H_2}) illustrate these behaviors of Hydrogen gas with a high diffusivity of $0.756 cm^2/s$ at 20°C spreads more slowly when entering areas with pollutants having lower diffusivities, such as carbon monoxide A_{CO}, B_{CO}, C_{CO}) and argon (A_{Ar}, B_{Ar}, C_{Ar}). Similarly, when argon ($\mu = 0.167 cm^2/s$) moves in, pollutants with higher diffusivities, like carbon monoxide and hydrogen, spread more slowly, leading to a gradual increase in pollutant concentration.

Concentration directly impacts space and time when the order of fractional derivatives changes while diffusion remains constant. Dispersion changes as fractional derivative orders change. Concentration spreading happens more quickly at higher orders. Higher fractional derivative orders imply stronger memory effects, potentially causing complex behavior like longer concentration tails and slower decay rates. Anomalous diffusion is influenced by fractional orders. Subdiffusion caused by smaller orders slows the concentration spread for a limited distribution. Greater orders indicate superdiffusive behavior, which accelerates the spread of concentration for a widely dispersed condition. The rate at which the material spreads out is influenced by changes in the diffusion coefficient, even while the order of fractional derivatives remains the same. It spreads more quickly with a greater diffusion coefficient, mitigating concentration disparities. Sharper concentration differences are maintained when the spreading is slowed down by a lower diffusion coefficient. It functions essentially like a dial to control how rapidly the perfume travels throughout space; the more diffusion, the faster and more evenly the smell spreads, and the less diffusion, the slower it spreads and may be longer concentrated in some locations.

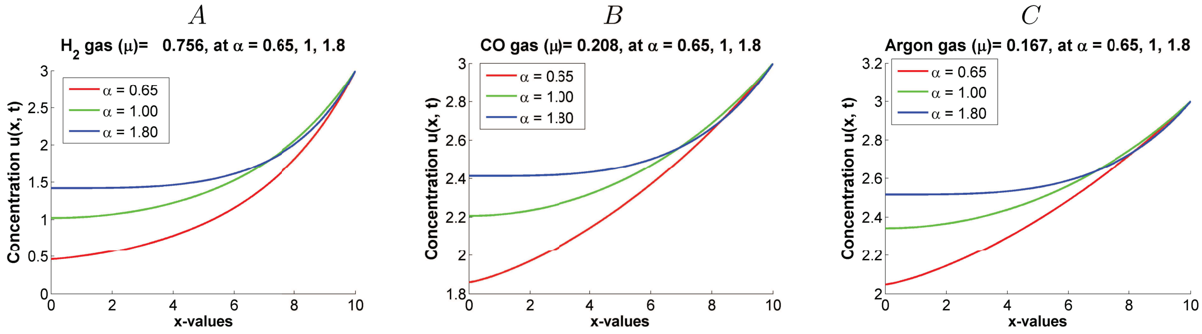

Figure 2: The solute concentration $u(x,t)$ in equation (8), A : H_2 gas: $\mu = 0.756$; B : CO gas: $\mu = 0.208$, and $C(\mathrm{Ar})$: $\mu = 0.167$, with varying fractional orders $\alpha = 0.65, 1, 1.8$.

Concentration of solutes $u(x,t)$ describes the distribution of pollutants over time and space. In subdiffusion ($0 < \alpha < 1$), pollutants disperse slowly due to obstacles like dense urban structures, vegetation, or barriers. In normal diffusion ($\alpha = 1$), pollutants spread in open areas, such as from a factory chimney, mixing gradually with the air. This model is suitable for rural or suburban environments with fewer obstructions. In superdiffusion ($1 < \alpha \leq 2$), pollutants are rapidly transported over large distances in high wind or turbulent areas, like highways or industrial zones, causing quick concentration changes.

3.2 Space-time fractional Advection Diffusion Equation

The following is an expression of space-time fractional advection-diffusion equation

$$\mathbb{D}_t^{\alpha} u = \mu \mathbb{D}_x^{2\beta} u - \mathbb{D}_x^{\beta} u \qquad (\text{for } \ \gamma = 2\beta) \ \ x, t > 0 \tag{9}$$

In air pollution, the Adomian's decomposition method is used for equation (9), with initial condition as $u(x,t) = e^{-x}$

$$u_{n+1} = \mu I^{\alpha}(\mathbb{D}_x^{2\beta} u_n) - I^{\alpha}(\mathbb{D}_x^{\beta} u_n)$$

Applying the recurrence relation yields the first five terms of u_n:

$$u_1 = \frac{t^{\alpha}}{\Gamma(\alpha+1)} \sum_{i=0}^{1} (-1)^i \begin{bmatrix} 1 \\ i \end{bmatrix} \mu^{(1-i)} \mathbb{D}_x^{(2-i)\beta} e^{-x},$$

$$u_2 = \frac{t^{2\alpha}}{\Gamma(2\alpha+1)} \sum_{i=0}^{2} (-1)^i \begin{bmatrix} 2 \\ i \end{bmatrix} \mu^{(2-i)} \mathbb{D}_x^{(2\times 2-i)\beta} e^{-x},$$

$$u_3 = \frac{t^{3\alpha}}{\Gamma(3\alpha+1)} \sum_{i=0}^{3} (-1)^i \begin{bmatrix} 3 \\ i \end{bmatrix} \mu^{(3-i)} \mathbb{D}_x^{(2\times 3-i)\beta} e^{-x},$$

$$u_m = \frac{t^{m\alpha}}{\Gamma(m\alpha+1)} \sum_{i=0}^{m} (-1)^i \begin{bmatrix} m \\ i \end{bmatrix} \mu^{(m-i)} \mathbb{D}_x^{(2\times m-i)\beta} e^{-x},$$

$$u(x,t) = \sum_{m=0}^{\infty} \frac{t^{m\alpha}}{\Gamma(m\alpha+1)} \sum_{i=0}^{m} \begin{bmatrix} m \\ i \end{bmatrix} \mu^{(m-i)} e^{-x} = e^{-x} E_{\alpha}(1+\mu) t^{\alpha}.$$

Under the initial condition $u(x,0) = e^{-x}$, the solution of the above equation reduces to (9) when $\beta = 1$. The space-time fractional advection-diffusion equation with γ=2β provides a simplified model for understanding how pollutants disperse in the air, taking into account both spatial and temporal dynamics. When the diffusion coefficient μ is very small, the equation behaves like a singularly perturbed problem [24], leading to unbounded solution derivatives and complicating error analysis. To address this, careful selection of numerical methods, appropriate mesh adjustment, and thorough stability analysis are essential. Kumar et al. [11] and Kumar et al. [12] have explored these issues, highlighting that small diffusion terms can lead to unbounded derivatives. For instance, the time FADE is $D_t^{\alpha} u = \mu D_x^2 u - D_x u$ and initial condition $u(x,0) = e^{-x}$ with unbouded derivatives: If we choose μ to be very small, the term $D_t^{\alpha} u$ become negligible compared to $-D_t^{\alpha} u$. Thus, $D_t^{\alpha} u \approx -D_x u$. We modify the initial condition for singularity: $u(x,0) = e^{-x} + \delta(x - x_0)$ where $x = x_0$ introduces the point source and δ is the Dirac delta. The soultion of fractional ADE can be written as,

$$u(x,t) = \frac{t^{\alpha}}{\Gamma(\alpha+1)} (e^{-x} - D_x(\frac{t^{\alpha}}{\Gamma(\alpha+1)} \delta(x - x_0)))$$

the term $D_x \delta(x - x_0)$ represents the derivative of the Dirac delta function, which is unbounded. The tables compare numerical and exact solutions for various fractional orders (α). The error decreases with increasing x, indicating higher accuracy at larger spatial positions. For $\alpha = 0.5$, the error drops from 0.0321 at $x = 0.30$ to 0.0004 at $x = 1.45$. For $\alpha = 1.8$, it reduces from 0.0131 to 0.0042 over the same range, suggesting greater accuracy for larger α. Careful handling is needed for precision and stability at small time scales ($t = 0.01$). Adding more terms to the Adomian decomposition method generally improves accuracy, as the series solution more closely approximates the exact answer. This results in reduced error, enhanced convergence, and increased stability. Since the Adomian Decomposition Method (ADM) is semi-analytical, its convergence analysis assumes compatibility conditions and solution smoothness within a fixed domain. Shakti et al. [26] and Das et al. have provided several alternative convergence assessments for this approach, as discussed in [6, 7, 8].

Table 1: H_2: $\mu = 0.756$, $\alpha = 0.5$ at $t = 0.01$

x	**Exact Solution**	**Numerical Solution**	**Error**
0.30	0.7539	0.7218	0.0321
0.50	0.6173	0.5858	0.0315
0.70	0.5054	0.4786	0.0267
0.90	0.4138	0.3937	0.0201
1.10	0.3388	0.3260	0.0127
1.20	0.3065	0.2974	0.0091
1.30	0.2774	0.2718	0.0055
1.40	0.2510	0.2489	0.0021
1.45	0.2383	0.2387	0.0004

Table 2: H_2: $\mu = 0.756$, $\alpha = 1.8$ at $t = 0.01$

x	**Exact Solution**	**Numerical Solution**	**Error**
0.30	0.7539	0.7408	0.0131
0.50	0.6173	0.6065	0.0108
0.70	0.5054	0.4966	0.0088
0.90	0.4138	0.4066	0.0072
1.10	0.3388	0.3329	0.0059
1.20	0.3065	0.3012	0.0053
1.30	0.2774	0.2725	0.0048
1.40	0.2510	0.2466	0.0044
1.45	0.2346	0.2387	0.0042

3.3 Space-time FADE ($0 < \beta \leq 1$) and ($1 < \gamma \leq 2$)

Given $u(x,0) = f(x)$ and for $0 < \alpha, \beta \leq 1$ and $1 < \gamma \leq 2$, the Adomian recursive terms for (9) are:

$$u_1 = \mu I^{\alpha}(\mathbb{D}_x^{\gamma} u_0) - I^{\alpha}(\mathbb{D}_x^{\beta} u_0) = \mu I^{\alpha}(\mathbb{D}_x^{\gamma} f(x)) - I^{\alpha}(\mathbb{D}_x^{\beta} f(x)) = \frac{t^{\alpha}}{\Gamma(\alpha+1)}[\mu \mathbb{D}_x^{\gamma} - \mathbb{D}_x^{\beta}] f(x),$$

$$u_2 = \frac{t^{2\alpha}}{\Gamma(2\alpha+1)}(\mu(\mathbb{D}_x^{\gamma}(\mu\mathbb{D}_x^{\gamma} - \mathbb{D}_x^{\beta}) - \mathbb{D}_x^{\beta}(\mu\mathbb{D}_x^{\gamma} - \mathbb{D}_x^{\beta}))f(x) = \frac{t^{2\alpha}}{\Gamma(2\alpha+1)}(\mu^2\mathbb{D}_x^{2\gamma} - \mu\mathbb{D}_x^{\gamma+\beta} - \mu\mathbb{D}_x^{\gamma+\beta} + \mathbb{D}_x^{2\beta})f(x).$$

Continuing, under the condition $\gamma = 2\beta$, the above relation reduces to

$$u_m(x,t) = [E_{\alpha}(t^{\alpha}(\mu\mathbb{D}_x^{2\beta} - \mathbb{D}_x^{\beta})]e^{-x}$$

and

$$u(x,t) = \sum_{m=0}^{\infty} \frac{t^{m\alpha}}{\Gamma(m\alpha+1)} \sum_{i=0}^{m} (-1)^i \begin{bmatrix} m \\ i \end{bmatrix} \mu^{(m-i)} \mathbb{D}_x^{(2m-i)\beta} e^{-x}.$$

If $\gamma = 2$, $\alpha = 1$, $\beta = 1$, and the following solution when we apply the initial condition $u(x,0) = e^{-x}$ to the classical advection diffusion equation: $u(x,t) = e^{-x+(1+\mu)t}$. The solution of a fractional advection-diffusion equation at a certain time t and position x is represented by the expression $u(x,t)$ which takes into account both the diffusion and advection processes in space as well as the memory effects in time. The non-local behavior is captured by the Mittag-Leffler function E_{α}, and the solution moves in space is determined by the combination of spatial derivative operators. This provides the precise solution to the problem. Setting the initial condition as $u(x,0) = x^n$, where n is any real exponent.

The space-time fractional advection-diffusion equation incorporates fractional derivatives in both spatial and temporal variables, extending traditional equations to encompass non-local and memory effects across both dimensions. The FADE provides a more comprehensive understanding of pollutant dispersion in the atmosphere by incorporating both spatial non-locality and temporal memory effects, leading to more accurate predictions and assessments of environmental impacts. The equation in the first image, which uses normal differential equations rather than fractional ones, shows a basic advection-diffusion process, which is often seen in scientific and technological disciplines, where $\alpha = \beta = n = 1$ and $\gamma = 2$. In the second image, the equation shows a system where advection functions as it would in a classical scenario, but the diffusion process exhibits fractional characteristics when $\beta = 1$ and $\alpha = 0.25$. This scenario might be typical of procedures where the diffusion process is impacted by long-range interactions or memory effects. Similarly, the third picture illustrates memory-dependent and non-local behavior with fractional characteristics in both the advection and diffusion processes at $\beta = 0.75$ and $\alpha = 0.5$. This scenario might represent systems where both advection and diffusion are influenced by long-range interactions or memory effects.

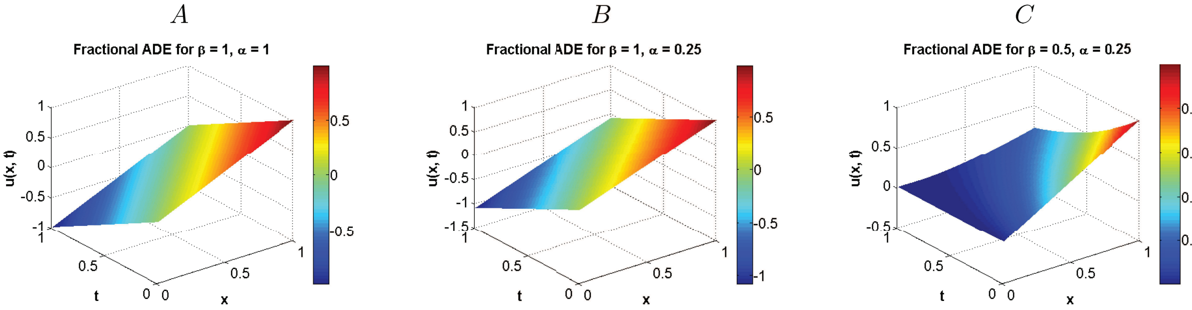

Figure 3: Solute concentration $u(x,t)$ for A: $\alpha = 1, \beta = 1$, B: $\alpha = 0.25, \beta = 1$, C: $\alpha = 0.25, \beta = 0.5$.

4 Conclusion

This work demonstrates the effectiveness of Adomian's Decomposition Method (ADM) in solving fractional advection-diffusion equations (FADE) with variable diffusivity and initial conditions, using Caputo fractional derivatives for time and variable-order derivatives for space. The solutions, expressed as an infinite series of Mittag-Leffler functions, reveal that higher fractional orders accelerate concentration spreading and increase memory effects while varying the diffusion coefficient adjusts the rate and uniformity of dispersion. Results indicate that varying diffusivity and the order of fractional derivatives significantly impact concentration profiles, with higher diffusion coefficients leading to faster, more uniform spreading. ADM proves robust for real-world scenarios with spatially varying diffusivity, providing valuable insights into systems with memory effects and heterogeneous diffusion. The ADM yields precise results, with errors decreasing as the fractional order α increases. Accuracy improves with higher spatial positions and more series terms. Graphical solutions confirm ADM's practical applicability. Fractional calculus's critical role in pollutant dispersion, where higher fractional orders α correspond to superdiffusion and faster spreading, and lower orders indicate subdiffusion and slower spreading. A one-dimensional model explores more general uses to improve the fractional diffusion process prediction capability.

Acknowledgements. Shankar Pariyar expresses gratitude to the University Grants Commission (UGC), Nepal, for providing financial support through the PhD fellowship (Award No. PhD-2025/26-S&T-13).

References

[1] B. Ahmad and A. Alsaedi, Solutions of the fractional advection dispersion equation with the modified Caputo derivative, Nonlinear Anal. Real World Appl., 16(2014), 14–23.

[2] M. Alneimat, M. Moakher, N. Djeddi and S. Al-Omari, Numerical solution of fractional model of Atangana-Baleanu-Caputo integrodifferential equations with integral boundary conditions, Appl. Math. E-Notes, 23(2023), 146–158.

[3] D. Baleanu and K. Diethelm, Fractional Calculus: Models and Numerical Methods, World Scientific, 2012.

[4] J. Bear, Modeling Phenomena of Flow and Transport in Porous Media, Theory and Applications of Transport in Porous Media, 31. Springer, Cham, 2018.

[5] R. Choudhary, S. Singh, P. Das and D. Kumar, A higher order stable numerical approximation for time-fractional non-linear Kuramoto-Sivashinsky equation based on quintic-spline, Math. Methods Appl. Sci., 47(2024), 11953–11975.

[6] P. Das, An a posteriori based convergence analysis for a nonlinear singularly perturbed system of delay differential equations on an adaptive mesh, Numer. Algorithms, 81(2019), 465–487.

[7] P. Das, A higher order difference method for singularly perturbed parabolic partial differential equations, J. Difference Equ. Appl., 24(2018), 452–477.

[8] P. Das, Comparison of a priori and a posteriori meshes for singularly perturbed nonlinear parameterized problems, J. Comput. Appl. Math., 290(2015), 16–25.

[9] P. Das, S. Rana and H. Ramos, On the approximate solutions of a class of fractional order nonlinear Volterra integro-differential initial value problems and boundary value problems of first kind and their convergence analysis, J. Comput. Appl. Math., 404(2022), 15 pp.

[10] S. Y. Huang, Bifurcation curves in Minkowski-curvature problem with nonlinearity $u^p + u$, Appl. Math. E-Notes, 23(2023), 544–559.

[11] S. Kumar, R. Ishwariya and P. Das, Impact of mixed boundary conditions and nonsmooth data on layer-originated nonpremixed combustion problems: higher-order convergence analysis, Stud. Appl. Math., 153(2024), 32 pp.

[12] K. Kumar, P. C. Podila, P. Das and H. Ramos, A graded mesh refinement approach for boundary layer originated singularly perturbed time-delayed parabolic convection diffusion problems, Math. Methods Appl. Sci., 44(2021), 12332–12350.

[13] S. Kumar, P. Das and K. Kumar, Adaptive mesh based efficient approximations for Darcy scale precipitation dissolution models in porous media, Internat. J. Numer. Methods Fluids, 96(2024), 1415–1444.

[14] F. Liu, P. Zhuang, L. W. Turner and V. Anh, Space-time fractional advection-dispersion equations with variable coefficients, Appl. Math. Model., 13(2003), 233–245.

[15] A. M. A. El-Sayed, S. H. Behiry and W. E. Raslan, Adomian's decomposition method for solving an intermediate fractional advection-dispersion equation, Comput. Math. Appl., 59(2010), 1759–1765.

[16] F. Mainardi, Fractional Calculus and Waves in Linear Viscoelasticity, An Introduction to Mathematical Models, Imperial College Press, London, 2010.

[17] H. M. Srivastava, A. K. Nain, R. K. Vats and P. Das, A theoretical study of the fractional-order p-Laplacian nonlinear Hadamard type turbulent flow models having the Ulam-Hyers stability, RRev. R. Acad. Cienc. Exactas Fís. Nat. Ser. A Mat. RACSAM, 117(2023), 19 pp.

[18] S. Pariyar, B. P. Lamichhane and J. Kafle, A time fractional advection-diffusion approach to air pollution: Modeling and analyzing pollutant dispersion dynamics, Partial Differential Equations in Applied Mathematics, 14(2025), 101149.

[19] S. Pariyar, and J. Kafle, Caputo-Fabrizio approach to numerical fractional derivatives, BIBECHANA, 20(2023), 126–133.

[20] S. Pariyar and J. Kafle, Generalizing the Mittag-Leffler function for fractional differentiation and numerical computation, Nepali Math. Sci. Rep., 41(2024), 1–14.

[21] Q. Rubbab, I. A. Mirza and M.-Z. A. Qureshi, Analytical solutions to the fractional advection-diffusion equation with time-dependent pulses on the boundary, AIP Adv., 6(2016), 7.

[22] S. Santra, J. Mohapatra, P. Das and D. Choudhuri, Higher order approximations for fractional order integro-parabolic partial differential equations on an adaptive mesh with error analysis, Comput. Math. Appl., 150(2023), 87–101.

[23] R. Shiromani, V. Shanthi and P. Das, A higher order hybrid-numerical approximation for a class of singularly perturbed two-dimensional convection-diffusion elliptic problem with non-smooth convection and source terms, Comput. Math. Appl., 142(2023), 9–30.

[24] S. Saini, P. Das, and S. Kumar, Parameter uniform higher order numerical treatment for singularly perturbed Robin type parabolic reaction diffusion multiple scale problems with large delay in time, Appl. Numer. Math., 196(2024), 1–21.

[25] S. Saini, P. Das and S. Kumar, Computational cost reduction for coupled system of multiple scale reaction diffusion problems with mixed type boundary conditions having boundary layers, Rev. R. Acad. Cienc. Exactas Fís. Nat. Ser. A Mat. RACSAM, 117(2023), 27 pp.

[26] D. Shakti, J. Mohapatra, P. Das and J. Vigo-Aguiar, A moving mesh refinement based optimal accurate uniformly convergent computational method for a parabolic system of boundary layer originated reaction diffusion problems with arbitrary small diffusion terms, J. Comput. Appl. Math., 404(2022), 16 pp.